MATERIALS RESEARCH COMMUNICATIONS
Vol. 1, No. 1 (2020) (11 pages)
@ Pusat Publikasi Ilmiah ITS

EVOLUTION OF STRUCTURE, PHASE AND MECHANICAL PROPERTIES DUPLEX STAINLESS STEEL (DSS) 31803 WELDING USING GMAW WITH THE ADDITION OF CO_2 TO Ar - CO_2 SHIELDING GAS

Hendra Butar Butar

Department of Materials and Metallurgical Engineering
Institut Teknologi Sepuluh Nopember,
Jl. Teknik Kimia, Keputih, 60111, Surabaya,East Java, Indonesia
endraboetar@gmail.com

Sulistijono*

Department of Materials and Metallurgical Engineering
Institut Teknologi Sepuluh Nopember,
Jl. Teknik Kimia, Keputih, 60111, Surabaya,East Java, Indonesia
ssulistijono@gmail.com

Agung Purniawan

Department of Materials and Metallurgical Engineering
Institut Teknologi Sepuluh Nopember,
Jl. Teknik Kimia, Keputih, 60111, Surabaya,East Java, Indonesia
agung-pur@mat-eng.its.ac.id

* **Corresponding author**

Abstract – The purpose of this study was to analyze the effect of CO2 on the composition of the Ar- CO_2 shielding gas in DSS 31803 duplex welding using GMAW on carbon deposition, ferrite fraction, microstructure, weld and HAZ mechanical properties. This study uses A (100% Ar), M1 (95% Ar + 5% CO_2), M2 (90% Ar + 10% CO_2), M3 (85% Ar + 15% CO_2), M4 (80% Ar + 20 % CO_2), M5 (75% Ar + 25% CO_2) and C (100% CO_2). From the results of the study, the microstructure of the weld metal in each specimen contained grain boundary austenite (GBA), Widmanstätten austenite (WA), intragranular austenite (IGA), and partial transformed austenite (PTA). Scanning electron microscopy (SEM) identifies the occurrence of chrome carbide precipitation (Cr23C6) HAZ region in specimens M5 and specimen C. The equilibrium phase of ferrite and austenite in weld metal areas is fulfilled in specimens A (34.8), M1 (38.9), M2 (36.4), M3 (38.4) and M5 (45.9). The highest average hardness value of vikers in weld metal area is found in M5 specimen which is 255 HV. While the lowest value in specimen C is 238 HV.The highest Vickers average hardness value in the heat affected zone (HAZ) is in specimen A which is 271 HV and the lowest hardness is in specimen C which is 245 HV. High tensile strength values are found in specimen M5 with value 800 MPA. While the value of low tensile strength in M4 specimens which is 652 MPA.

Keywords: Duplex Stainless Steel, GMAW welding, shielding gas, measurement of volume fraction

1. Introduction

Increased applications in many industries such as shipbuilding, offshore, chemical industry, paper and pulp industries, petrochemicals, desalination plants, oil and gas industries are increasingly introducing DSS to the wider world (Verma and Taiwade, 2016; Ramkumar et al., 2016). Duplex stainless steel (DSS) is one of the special stainless steels because it has a microstructure of γ-austenite (face center cubic) and δ-ferrite (body center cubic) which is almost the same or 50% ferrite and 50% austenite so that it has a mechanical strength value high and excellent corrosion resistance properties. Welding is one of the fabrication processes that cannot be avoided

in most DSS applications. Even though they have good welding capability, the welding process can disturb the volume fraction balance between the two phases. The austenite content in the fusion and weld area must be in the range of 30% - 70% or 35% - 65% (ISO 15156, 2015; NORSOK M-601, 2016). When there is an imbalance in the volume fraction between the ferrite and austenite phases, it is possible to form nitrides, carbide precipitation, and sigma phases in the heat affected zone (Sadeghian et. al., 2014). Therefore, the formation of destructive phases should be avoided so that the mechanical properties and corrosion resistance are maintained. (Karlsson, 2012).

Tungsten gas arc welding (GTAW) is one of the best welding techniques for connecting DSS because it produces high-quality welded joints (Chern et al., 2011). Although welding of tungsten gas (GTAW or TIG) can be used to weld all types of metals, GTAW has the disadvantage of being a very low weld deposititon rate (0.9 - 1.8 kg/h) and the welding process of thick workpieces takes a long time so resulting in slow productivity. Therefore GTAW is more suitable for thin metal welding. In this situation GMAW welding is used because the weld deposititon rate produced is very high (2.6 - 4.5 kg/h) so that productivity is faster than that of GTAW and SMAW where the SMAW weld deposition rate is in the range of 1. 5 - 3 kg/h (Avesta Welding Manual, 2004; Kou, 2003). In GMAW welding there are several parameters used, namely; current, voltase, welding speed, heat input, filler metal selection, metal transfer mode, fill wire speed, nozzle distance from workpiece, welding position, and protective gas (Rizvi and Tewari, 2017; Gill and Singh, 2012). Shielding gas used in welding GMAW especially in duplex stainless steel is a mixture of argon (Ar) - carbon dioxide (CO_2), argon (Ar) - oxygen (O_2), and argon (Ar) - helium (He) - carbon dioxide (CO_2). But the shielding gas mixture is used to a certain extent to obtain the results that are desired as desired (Avesta Welding Manual, 2004). The main function of the shielding gas in the GMAW welding process is to protect the welding pool from contamination of the surrounding atmosphere and arc stabilizers. Munez et al., (2010) in welding GMAW duplex stainless steel with a composition of 98% Ar - 2% CO_2 found that the ferrite phase and the austenite phase were in balance with 45% - 55% and showed a good crab corrosion resistance and had a high hardness value. The hardness value of the weld metal can vary with changes in the composition of the shielding gas CO_2. This is due to the presence of carbon elements in the CO_2 protective gas. However, tensile and elongation strength decreased from 613 MPA to 610 MPA along with increasing CO_2 in the shielding gas mixture of 2-20% (Liao and Chen 1999). The protective gas by using pure argon is more directed to the mechanical properties of the weld metal. The highest hardness and toughness was found in 100% Ar, while in the CO_2 shielding gas mixture of 5%, 10%, 20% and 100% CO_2 experienced a decrease in mechanical properties. Nevertheless,carbon dioxide is the preferred shielding gas for steel metal arc (GMAW) welding because it offers advantages such as higher welding speed, greater penetration and lower price. However, the use of pure CO_2 is limited because of problems associated with large spatter sparks and elemental losses due to oxidation.

This research studies the effect of carbon dioxide on the composition of Ar - CO_2 shielding gas on microstructure, phase equilibrium and mechanical properties of weld metal and HAZ on welding 38103 duplex stainless steel using GMAW method.

2. Experimental Method

This research uses parent metal with DSS material ASTM A790M 2205 UNS S31803. The size of the material used is a 4 "NPS diameter pipe with a thickness of 6.02 mm (Sch. 40S). The filler wire (filler metal) used is ESAB OK Autrod 2209 1.2 mm in diameter. OK Autrod 2209 has high corrosion resistance. The chemical composition of the parent metal and parent metal can be seen in table 1.

Tabel 1. Chemical composition of base metal and filler wire

Materials	Chemical composition (wt%)							
	C	Cr	Ni	Mo	N	Mn	Cu	Si
Base Metal	0.021	22.4	5.1	3.1	0.16	1.06	0.2	0.4
OK Autrod 2209	0.025	23.5	9.5	3.5	0.2	1.8	0.2	0.65

DSS welding material specimens is carried out using machining processes, cutting machines, and lathes. The seam design uses a single V Groove type full penetration with a slope of ± 30 °. The root face test piece is made of ± 2 mm and uses a root opening of 2 mm. The design of the welding joint can be seen in figure 1.

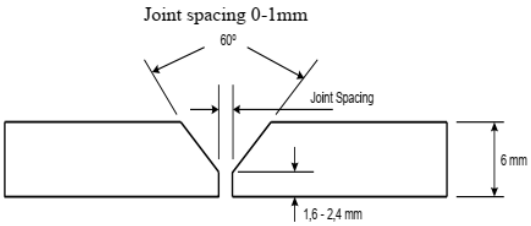

Fig. 1. Design joint

Welding of duplex stainless steel using GMAW welding with shielding gas composition, among others; 100% Ar, 95% Ar + 5% CO_2, 90% Ar + 10% CO_2, 85% Ar + 15% CO_2, 80% Ar + 20% CO_2, 75% Ar + 25% CO_2 and 100% CO_2. Shielding gas flow rate settings of 10-20 ltr / min. The welding position used in this study is 1G by string and weave. In welding duplex stainless steel pipes, using pure argon gas backing> 99.5%. Gas backing flow rates are set at 15-25 l / min. The welding parameters can be seen in table 2.

Table 2. Welding parameters using GMAW

Welding Process	***Polarity***	***Current (A)***	***Voltage (V)***	***Travel speed (mm/min)***	***Heat input (kJ/mm)***
GMAW	DCEP	110-150	15-20	70- 120	1.4-1.5

Before conducting micro-analysis, the cut specimens are then grinding and polishing. Grinding technique is done by rubbing the specimen with scouring paper from grid 200 to grid 2000. DSS 31803 welding specimens are etched electronically or electrochemically by using a solution of 10 g oxalid acid (oxalid acid) in 100 mL aquades with a potential of 2V for 15-30 seconds (Zhang et. al, 2016) and dried with a hair dryer. The microstructure of the weld metal and the heat affected zone (HAZ) were observed with optical microscopy and scanning electron microscopy (SEM). The volumetric ferrite fraction in the weld area was measured using the Feritscope FMP30 so that the results were more accurate.The vickers hardness test is performed at 3 points in the HAZ region vertically, 3 points on the weld metal horizontally and 3 points at the parent metal horizontally. Tensile testing is adjusted to the testing standard JIS Z 2201 (1998) (test rod no. 12 B) which refers to ISO 6892 (1984).

3. Results and Discussion

3.1 Microstrucrure

After the welding process, the microstructure of each specimen was observed with an optical microscope in the area of heat influence (HAZ) and weld metal with a magnification of 200x, 500 x and 1000x (figure 2a and 2b). The rate of cooling and nickel-enriched filler metals play a major role in the evolution of the microstructure of welding metals. Weld metal areas and heat affected zones (HAZ) which experience slow cooling rates at the ferrite solvus temperature, will form fewer ferrite phases than the base metal area. In figure 2a, welding using pure Ar protective gas or without CO_2 in the protective gas, the ferrite matrix is almost covered by austenite phase which is large enough so that the ferrite phase decreases and the austenite phase increases. This is due to

the rapid cooling rate so that the ferrite phase does not have enough time to fully transform into austenite. An almost closed ferrite matrix was also found with the addition of 10%, 15%, 20%, 25% and 100% CO_2 (figure 2a and 2b). But with the addition of 5% CO_2 in the protective gas, a sufficiently balanced phase is obtained in the weld metal where the austenite phase does not all cover the ferrite matrix (figure 2a). This is because the ferrite phase experiences a rapid cooling rate so that it can transform into the austenite phase quite perfectly and the CO_2 composition added to the protective gas is quite small. The austenite phase is relatively dense and complex in welding metals, because the Ni and N content in chemical compositions of filler wires is quite high at 9.5% Ni and 0.2% N, higher than base metals.

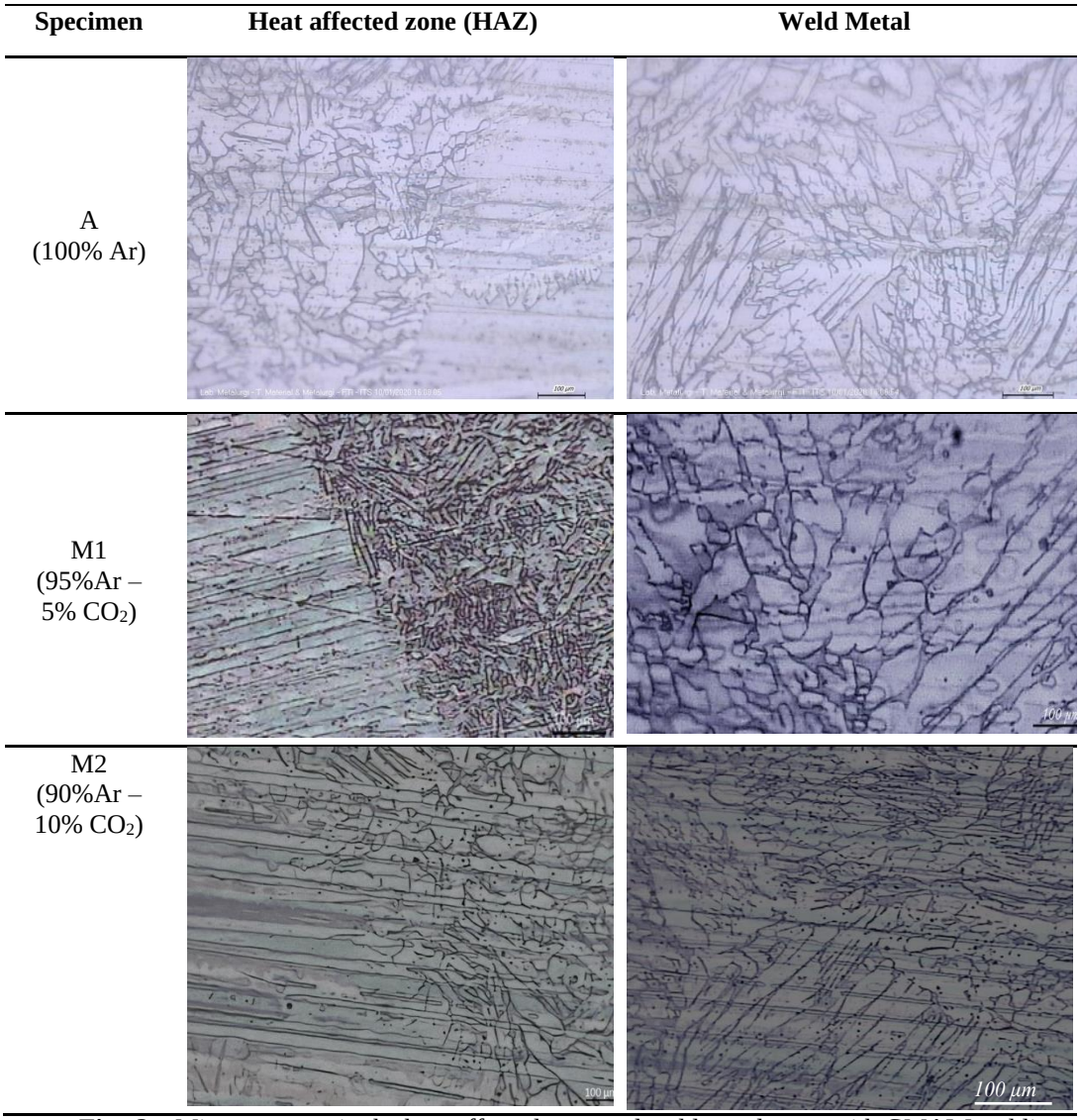

Fig. 2a. Microstructure in the heat affected zone and weld metal areas with GMAW welding which is etched electrochemically in 10% wt oxalic acid 15-20 seconds.

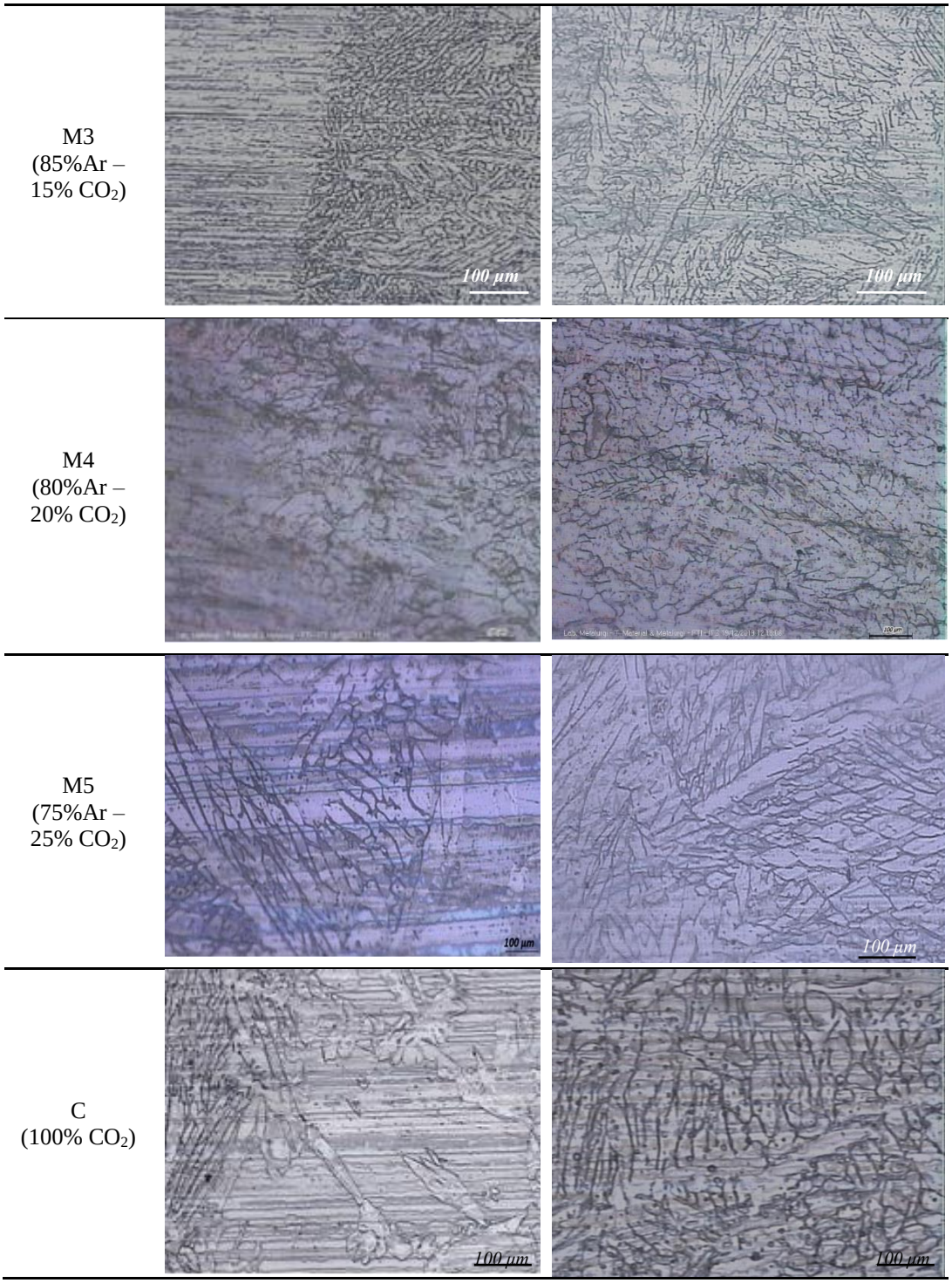

Fig. 2b. Microstructure in the heat affected zone and weld metal areas with GMAW welding which is etched electrochemically in 10% wt oxalic acid 15-20 seconds.

During deposition or solidification in the welding process, austenite can be divided into two types namely primary austenite (γ1) and secondary austenite (γ2). Primary Austenite (γ1) is immediately compacted from

liquid metal in the process of solidification (L → γ1 and L + α → γ1) and the subsequent solid state phase transition from ferrite to γ1 (α → γ1), which contains grain boundary austenite (GBA), Widmanstätten austenite (WA), intragranular austenite (IGA), and partial transformed austenite (PTA). Allotriomorphic grain boundary autenite (GBA) begins to nucleate and grow at the α / α limit. Nucleated grain boundary austenite (GBA) occurs in the cooling temperature range of 1350–8000C (Eghlimi et. al., 2014). When cooling continues, the amount of GBA increases so that the nucleation that occurs at the α / α limit decreases and new nuclei begin to form at α / γ interfaces. The new austenite nucleus formed at the α / batas boundary grows toward the ferrite in the form of Widmanstätten austenite (WA) side plates (Ramirez et al., 2004). Widmanstätten austenite (WA) is formed from heating duplex stainless steels at a low temperature range of 650-800 ° C. Widmanstätten austenite (WA) items are formed from GBA. Although Ni is enriched compared to ferrite matrices but has a lower amount of Cr, Mo, and nitrogen content than GBA (Sieurin and Sandstrom, 2006). Intragranular austenite (IGA) is deposited in areas rich in Cr / Mo and rich in Ni / N in metastable ferrite. Formation of IGA in ferrite grains requires long cooling compared to GBA and WA because it has high activation energy for lattice diffusion. The temperature range of the occurrence of intergranular austenite is at 1000-1100 ° C. IGA is generally formed through heterogeneous nucleation at inclusions and dislocations or in intragranular deposits. Intragranular austenite (IGA) has finer grains compared to GBA and WA because lattice diffusion is slower in ferrite than at its own grain boundary. Most of the austenite dissolves after the heating process is adjacent to the double phase area (α + L), as in multi-pass welding. However, small amounts of austenite remain in ferrite, so it is called partial transformed austenite (PTA). Partial transformed austenite (PTA) occurs at 1345 ° C where most of the austenite has been separated from δ-ferrit (Yang et al., 2011). Partial transformed austenite (PTA) also has an important influence in effectively inhibiting the separation of Cr and Mo at solidus temperatures, it also inhibits the growth of ferrite grains (Eghlimi et al., 2015). In addition, the micro structure of the welding heat affected zone (HAZ) consists of large and coarse ferrite grains with low austenite content. This is due to the presence of nitrides that are rich in chromium, carbides and other intermetallic compounds.

The GMAW process with a 100% CO_2 shielding gas composition facilitates the formation of more austenite in the weld metal area compared to GMAW with Ar as a protective gas (figure 3). This is because there is a carbon element in the CO_2 shielding gas where carbon is one of the elements forming austenite, thus facilitating the austenite phase more than the ferrite phase.

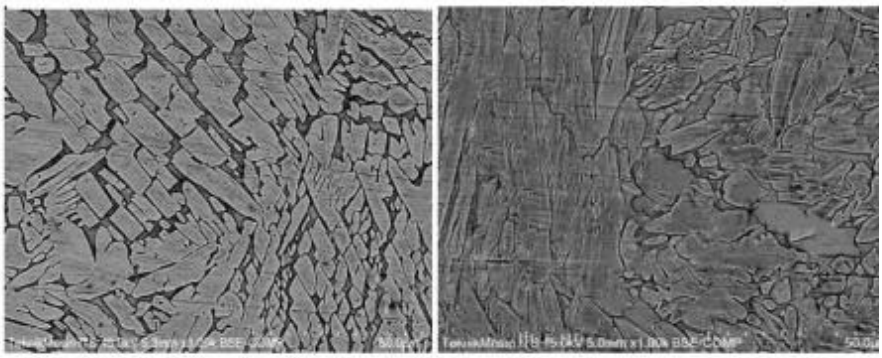

Fig 3. Scanning electron microscopy (SEM) weld metal area (a) 100% Ar and, (b) 100% CO_2 with a magnification of 1000x

3.2 Chrome carbide identification

In figure 4, it is identified that there is a chrome carbide precipitation in the HAZ region. Chromium carbide precipitation is influenced by the presence of high carbon content during slow cooling between temperatures of 800^0C to 550^0C and is most formed in HAZ which will bind chromium in the grain boundary region or ferrite-austenite interface, so that the chromium content is reduced. The emergence of chrome carbide is usually when given heat treatment. The carbon element in the CO_2 shielding gas greatly influences the precipitation at the α / γ

grain boundary. The increasing composition of CO_2 in the protective gas makes the carbon element out of the weld metal. In this study, Cr23C6 compounds analyzed by EDX showed that chromium became the largest element up to 23.93 wt% for the addition of 25% CO_2 and 23.55 wt% with 100% CO_2 as a protective gas. in other words there is no special relationship between carbides and phasesδ-ferit using EDs analysis.

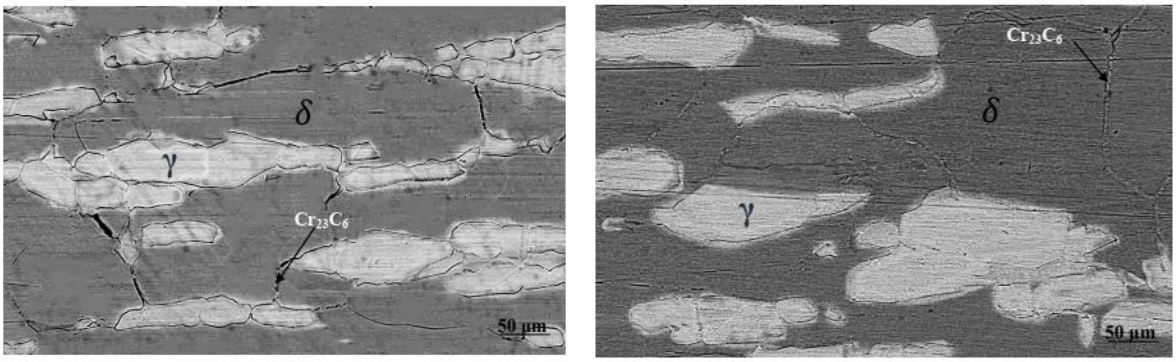

(a) (b)

Fig. 4. Scanning electron microscopy (SEM) area HAZ (a) 75% Ar + 25% CO_2 and, (b) 100% CO_2 with a magnification of 1000x

This is in line with what was done by Kwang Min Lee et al, (1999), where the chrome element was found at 23 wt%. Carbide precipitation in the limitδ/ γ has high chromium content, which causes thinning of chromium from around the boundary in ferrite. This will be the driving force for the growth of the austeniteδ-ferite and because the chromium region that has been depleted of ferrite will turn into secondary austenite, while the area around secondary austenite has a high chromium content after growth γ2 expands the excess chromium content to the boundary near ferrite Nuclear phenomena and Cr23C6 carbide growth accompanied by migration initial grain boundary α/γ into phaseδ-ferrite. Precipitation of Cr23C6 carbides is most common by decreasing the solubility of carbon and nitrogen in austenite. When the ferrite decomposition begins, precipitation of the α/γ carbide interface boundary occurs first by the eutectoid reaction.

3.3 Measurement of volume fraction phases ferrite - austenite

The austenite content in the weld metal area must be at 30% - 70%. Ferrite% is a parameter used to indicate the presence of delta ferrite. The amount of ferrite in deposite weld metal is determined by the chemical composition of the filler metal and base metal, welding process, shielding gas type, welding procedure and heat input. The equilibrium phase of ferrite and austenite bada weld metal is fulfilled in the range of 30% - 70% in specimens with the addition CO_2 in shielding gas 5%, 10%, 15%, 25% except for specimens with the addition of 20% CO_2 which has a ferrite content value of 25, 8 (table 3). The use of 100% argon shielding gas has a ferrite value of 34.8 higher than using 100% C02, which is 24.4. 25% increase CO_2 into the protective gas Ar - CO_2, has the highest ferrite value than other gas mixtures. This is due to the presence of carbon in the protective gas CO_2, where the carbon element is one of the elements forming austenite. In addition, the austenite Ni forming and stabilizing elements obtained from metal fillers / fillers are 9% wt higher than base metals about 5% wt. After welding, the ferrite delta undergoes solidification, and after the solidification process is complete, the ferrite transforms into austenite through solid phase transformation. However, cooling after welding is too fast to allow austenite content to approach equilibrium level. The weld metal area and heat affected zone (HAZ) which experience slow cooling rates at the ferrite solvus temperature, will form less ferrite phase than the base metal area. However, if rapid cooling occurs, weld metal areas and DSS heat-affected zones produce ferrite-austenite phases tend to be more equilibrium than slower cooling. Increased composition CO_2 in shielding gases and slow solidification can also reduce the percentage of ferrite (Liao and Chen, 1998). Carbon and nickel are one of the

strongest formers of austenite. Carbon and nickel will increase as the composition increases CO_2 in shielding gas.

Table 3. Ferrite content (% Ferrite) in welding Duplex Stainless Steel (DSS) 31803

Spesimen	***Shielding Gas***	***Weld Metal*** **(% Ferit)**
A	Ar UHP	34.8
M1	95%Ar + 5%CO_2	38.9
M2	90%Ar + 10%CO_2	36.3
M3	85%Ar + %15CO_2	38.4
M4	80%Ar + 20%CO_2	25.8
M5	75%Ar + 25%CO_2	45.9
C	100%CO_2	24.4

3.4 Hardness (Vickers Hardness)

Hardness testing uses the vickers hardness method using SNI 8390: 2017 which refers to ASTM E92: 2004. From figure 5, the lowest hardness value in the parent metal is found in the specimen with 90% Ar + 10% CO_2 shielding gas which is 253 HV. And high hardness was found in the 85% Ar + 15% CO_2 specimen, 258 HV. The hardness of a DSS parent metal depends on the individual austenite phase and the ferrite present in the microstructure. The highest vikers hardness value of weld metal was found in the 75% Ar + 25% CO_2 specimen, 255HV, while the lowest value was found in the specimen with 100% CO_2, 238 HV. This is due to the increase in the composition of CO_2 into the protective gas, thereby increasing the carbon content in the weld metal. Then filler metal or filler wire has higher ferrite forming elements or elements to increase the hardness value such as Cr and Mo in the welded joint.

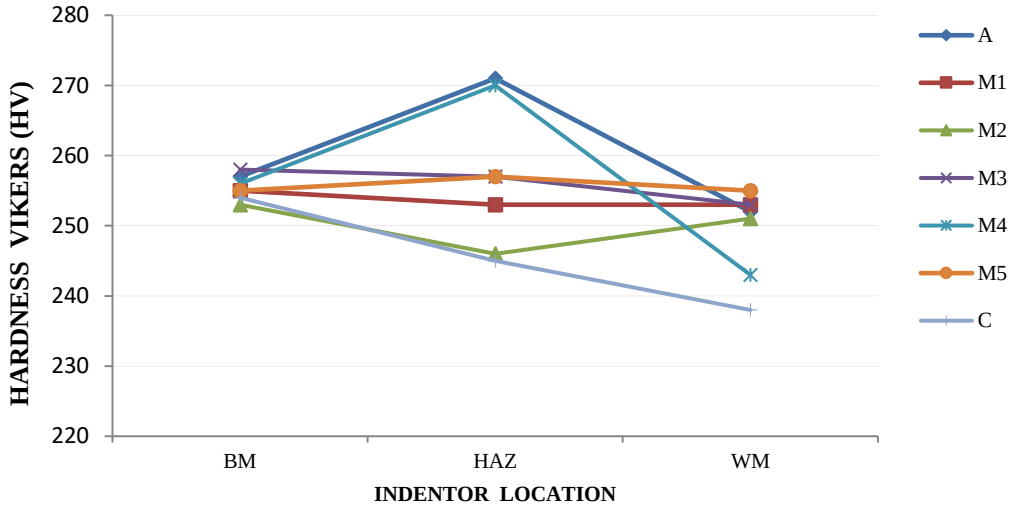

Fig. 5. The distribution of Vickers hardness averaged based on the location of the indentation.

When compared to the parent metal area, DSS welding metals provide higher hardness due to stresses caused by hardening during the welding solidification process, fast thermal cycles, and residual stress formation in welds. The highest Vickers hardness value in the heat affected zone (HAZ) area is found in the specimens using 100% Ar protective gas which is 271 HV. While the lowest hardness value is found in the 100% CO_2 shielding gas which is 245 HV. In welding duplex stainless steel (DSS) shows that the value of hardness is higher than the welding metal and its parent metal in the HAZ region. This is caused by the presence of coarse grain ferrite in the HTHAZ area so that it leads to higher violence. The presence of secondary phases such as sigma-σ, nitride, and carbide in the HAZ region can cause an increase in the value of DSS hardness.

3.5 Tensile strength

Duplex Stainless Steel UNS 31803 welding tensile testing using GMAW with the addition of CO_2 into the shielding gas, obtained the highest tensile strength value of 800 MPA on 75% Ar + 25% CO_2 shielding gas. While the lowest tensile strength value using 80% Ar + 15% CO_2 is 652 MPA (fig.6). Decreasing the value of the tensile strength of this test is the discovery of the type of welding defect slag (trapped slag). Slag inclusion is an oxide and other non-metal objects that are trapped in the welding metal. As a result, the strength of the weld joint will be reduced. The increase in tensile strength is also due to the high levels of the element nickel in the filler wire which exceeds the parent metal. Addition of 9% nickel to the filler metal thereby adding to the higher austenite content in the fusion zone. The choice of filler metal plays a major role in determining the tensile strength of welds. The use of filler metal enriched nickel ER 2209 makes the tensile strength of weld metal exceeds the tensile strength of the parent metal and maintains its tenacity.

Fig. 6. The effect of shielding gas on the value of the tensile strength with using GMAW

4. Conclusion

The microstructure of the weld metal in each specimen contained grain boundary austenite (GBA), Widmanstätten austenite (WA), intragranular austenite (IGA), and partial transformed austenite (PTA). An almost closed ferrite matrix was found with the addition of 10%, 15%, 20%, 25% and 100% CO_2. This is caused by the rapid cooling rate so that the ferrite phase does not have enough time to transform into austenite completely. The chrome carbide precipitation is affected by the presence of high carbon content and occurs during temperature sensation of 800^0C to 550^0C and most formed in HAZ which will bind chromium at the boundary area of the grain or interface (α/γ) ferrite - austenite, so that the chrome content around the ferrite is

depleted. This equilibrium-austenite phase equilibrium occurs due to the rapid cooling rate of the DSS weld metal area so that the ferrite-austenite phase tends to be more equilibrium than slower cooling. Also influenced by high levels of austenite-forming elements in filler wires such as Ni, N, C and Mn. The highest average hardness value of vikers in weld metal area is found in M5 specimen (75% Ar + 25% CO_2) which is 255HV, while the lowest value is found in specimens with 100% CO_2 which is 238 HV. While the highest Vickers hardness value in the heat affected zone (HAZ) is found in the specimens using 100% Ar shielding gas which is 271 HV and the lowest hardness is in 100% CO_2 protective gas which is 245 HV. This is caused by the presence of coarse grain ferrite in the HTHAZ area so that it leads to higher hardness. The highest tensile strength value was found in specimen M5 (75% Ar + 25% CO_2) with a value of 800 MPA. The increase in tensile strength is also due to the high levels of the element nickel in the filler wire which exceeds the parent metal and the increased carbon element in the weld metal due to an increase in CO_2 shielding gas. While the decrease in the value of tensile strength due to slag inclusion welding defects thereby reducing the strength of the weld joint.

Acknowledgments

This writer would like to thank several parties who have provided support, guidance, and opportunities to the author so that this research can be completed.

References

ASTM E92, Standard Test Method for Vickers Hardness of Metallic Materials

Avesta Welding Manual (2004), Practice and Products For Stainless Steel Welding. Avesta Welding, Swedia.

Eghlimi, A. Shamanian, M. Raeissi, K. (2014), "Effect of current type on microstructure and corrosion resistance of super duplex stainless steel claddings produced by the gas tungsten arc welding process", *Surface Coating Technology*, Vol. 244, pp.45–51

Gill, J dan Singh, J. (2012), "Effect Of Welding Speed And Heat Input Rate On Stress Concentration Factor Of Butt Welded Joint Of Is 2062 E 250", *International Journal of Advanced Engineering Research and Studies*, Vol. I(III), pp. 98–100.

ISO 15156., (2015). ISO 15156-3:2015, Petroleum and natural gas industries — Materials for use in H2S-containing environments in oil and gas production — Part 3: Cracking-resistant CRAs (corrosion-resistant alloys) and other alloys (Vol. 3).

JIS Z 2201, (1998) Test pieces for tensile for metallic materials, Japanese Standard Association.

Karlsson, L.(2012), "Welding Duplex Stainless Steels — A Review Of Current Recommendations. Welding in the World, Vol. 56, No. (5–6), pp. 65–76.

Kwang Min Lee , Hoon Sung Cho, Dap Chun Choi. (1999), "Effect of isothermal treatment of SAF 2205 duplex stainless steel on migration of α/γ interface boundary and growth of austenite", *Journal of Alloys and Compounds*, Vol.285, pp. 156–161

Kou, S. (2003), Welding metallurgy, 2nd edition. Wiley-Interscience, Hoboken

Liao, M and Chen, W. (1998), "The Effect of Shielding-Gas Compositions On The Microstructure and Mechanical Properties of Stainless Steel Weldments", *Materials Chemistry and Physics*, Vol. 55, No. 2, pp, 145-151.

Liao, M and Chen, W. (1999), " A Comparison of Gas Metal Arc Welding With Flux-Cored Wires and Solid Wires Using Shielding Gas", *International Journal of Advanced Manufacturing Technology*, Vol. 15, No. 1, pp. 49–53

Munez, CJ, Utrilla, MV, Urena, A, Otero, E. (2010), "Influence of the filler material on pitting corrosion in welded duplex stainless steel 2205". *Welding International*, Vol. 24, pp.105–110

NORSOK M-601. (2016), Welding and Inspection of Piping, Norwegian Oil and Gas Association and The Federation of Norwegian Industries.

Ramirez, A. J., Brandi, S. D., & Lippold, J. C., (2004), "Secondary austenite and chromium nitride precipitation in simulated heat affected zones of duplex stainless steels", *Science and Technology of Welding and Joining*, Vol. 9(4), pp,301–313.

Ramkumar KD, Goutham PS, Radhakrishna VS, Tiwari A, Anirudh S. (2016), "Studies on the structure property relationships and corrosion behaviour of the activated flux TIG welding of UNS S32750", *Journal of Manufacturing Processes*, Vol. 23, pp. 231–241.

Rizvi, S. A., and Tewari, S. P. (2017), "Multi Objective Optimization by Application of Taguchi Based Grey Relational Analysis for GMA Welding of IS2062 Structural Steel"**,** *Mechanics and Mechanical Engineering*, Vol. 21, No. 3, pp. 717–729.

Sadeghian, M., Shamanian, M., & Shafyei, A., (2014), "Effect of heat input on microstructure and mechanical properties of dissimilar joints between super duplex stainless steel and high strength low alloy steel". *Materials & Design*, Vol. 60 (Supplement C), pp. 678–684.

Verma, J. and Taiwade, RV.(2016), "Dissimilar welding behavior of 22% Cr series stainless steel with 316L and its corrosion resistance in modified aggressive environment". *Journal of Manufacturing Processes*, Vol. 24, pp.110.

Yang, Y.H., Yan, B., Li, J., Wang, J. (2011) "The effect of large heat input on the microstructure and corrosion behaviour of simulated heat affected zone in 2205 duplex stainless steel", *Corrosion Science*, Vol. 53, pp. 3756–3763

Zhang, Z., Jing, H., Xu, L., Han, Y., & Zhao, L. (2016), "Investigation On Microstructure Evolution And Properties Of Duplex Stainless Steel Joint Multi-Pass Welded By Using Different Methods", *Materials & Design*, Vol. 109, pp, 670–685.